https://doi.org/10.5194/egusphere-2023-1361
Preprint. Discussion started: 26 June 2023

Amazonian Aerosol Size Distributions in a Lognormal Phase Space: Characteristics and Trajectories

Gabriela R. Unfer[1,2,3], Luiz A. T. Machado[2,3], Paulo Artaxo[2], Marco A. Franco[2,4], Leslie A. Kremper[3], Mira L. Pöhlker[3,5,6], Ulrich Pöschl[3] and Christopher Pöhlker[3]

[1]Center for Weather Forecasting and Climate Research, National Institute for Space Research (INPE), Cachoeira Paulista, 12630-000, Brazil.
[2]Institute of Physics, University of São Paulo (USP), São Paulo, 05508-090, Brazil.
[3]Multiphase Chemistry Department, Max Planck Institute for Chemistry (MPIC), Mainz, 55128, Germany.
[4]Department of Atmospheric Sciences, Institute of Astronomy, Geophysics and Atmospheric Sciences (IAG), University of São Paulo, São Paulo, 05508-090, Brazil.
[5]Atmospheric Microphysics Department, Leibniz Institute for Tropospheric Research (TROPOS), Leipzig, 04318, Germany.
[6]Faculty of Physics and Earth Sciences, Leipzig Institute for Meteorology, Leipzig University, Leipzig, 04103, Germany.

Correspondence to: Luiz A. T. Machado (l.machado@mpic.de) and Christopher Pöhlker (c.pohlker@mpic.de)

Abstract. This study introduces a new approach to represent and analyse particle number size distributions (PNSD) of atmospheric aerosols. Amazonian aerosol data, measured from May 2021 to April 2022 at the Amazon Tall Tower Observatory (ATTO), were fitted by a trimodal lognormal function and the outputs were evaluated by means of the N-D_g-σ phase space. This is a 3D space defined by the three fit parameters of the lognormal function, which represents, for a given mode i, the number concentration (N_i), the geometric median diameter ($D_{g,i}$), and the geometric standard deviation (σ_i). Each state of a PNSD is represented by a single dot in this phase space, while a collection of dots shows the delimitation of all PNSD states under given conditions. The connections in ensembles of data points show trajectories caused by pseudo-forces, such as precipitation regimes and vertical movement. Characteristic patterns of the Amazonian PNSDs were found in the N-D_g-σ phase space, including the sub-50 nm mode appearing as a curved cone, the Aitken mode as a semi-sphere, and the accumulation mode as a cylinder. The trajectories of the data points as a function of seasonal and diel trends occur as well-defined paths. An ellipsoid pattern describes all possible seasonal states PNSDs of the accumulation mode. The diurnal cycle of sub-50 nm particles in the dry season shows a positive linear slope as a function of all three fit parameters. For wet and dry seasons, the diurnal cycle in the accumulation mode is mainly driven by changes in N. As an effect of precipitation on the PNSDs and vice-versa, N and D_g were found to increase for the sub-50 nm mode and to decrease for the Aitken and accumulation modes after the precipitation peak. While afternoons with precipitation were preceded by mornings with larger particles of the accumulation mode, whose mean geometric diameter was ~10 nm larger than in days without precipitation. Nevertheless, only in the wet season both concentration and diameter seem to influence further rainfall. Observed patterns of the PNSDs in the N-D_g-σ phase space can support the characterization of atmospheric aerosols e.g. in comparisons of different measurement sites, contribute to our understanding of the main processes in aerosol-cloud interactions, and open new perspectives on aerosol parametrizations. This study introduced a first glance of Amazonian aerosols in an N-D_g-σ phase space.

https://doi.org/10.5194/egusphere-2023-1361
Preprint. Discussion started: 26 June 2023

1 Introduction

Representing the interactions between atmospheric aerosols and clouds is one of the major challenges in climate and Earth systems models (Forster et al., 2021). Aerosols are a key factor for cloud formation and properties (Albrecht, 1989; Koren et al., 2005; Rosenfeld et al., 2008; Heikenfeld et al., 2019), while weather events are one of the main drivers in controlling aerosol concentration (Machado et al., 2021).

Extended time periods and high spatial resolution simulations are associated with significant computational costs, especially if sophisticated parametrizations of the aerosol-cloud interactions are being applied. Therefore, certain processes are generalized, particularly at the expense of resolving aerosol and cloud processes (Roesler & Penner, 2010), whose generalization sometimes provides only the total particle or droplet number concentrations. By applying sensitivity tests in Amazonian warm-phase clouds, it was shown that the intensity of droplet activation is mostly influenced by a variation in diameters and standard deviations of the particle number size distribution (PNSD), rather than by the total number concentration (Hernández Pardo et al., 2019). Improving aerosols parameterizations by allowing the employment of their characteristics, rather than generalizations, at the same time computational cost is not significantly increased, is one of the ways to better represent aerosol-cloud interactions. One possible strategy for approaching this issue can emerge from better representations of the PNSDs themselves.

Working with PNSDs enables a statistical representation of an ensemble of particles and its spatiotemporal variability. Multiple models are useful for describing PNSDs, such as gamma (Ulbrich, 1983) or lognormal (Aitchison and Brown, 1957) distribution functions. There is no definite consensus on which model best describes aerosol particles, as documented by an ongoing debate (Williams, 1985; Wu and Mcfarquhar, 2018, Nyaku et al., 2020). Nevertheless, the lognormal distribution is widely used in aerosol and related communities, mainly due to its simplicity (Pöhlker et al., 2021). The lognormal distribution is described by its moments, the geometric mean or median diameter (D_g), and the standard deviation (σ), describing and fitting different PNSD shapes, which includes multi-modal distributions (Heintzenberg, 1994).

The microphysical properties of an aerosol population, such as the particle fraction acting as cloud condensation nuclei (CCN), depend on particle size (D_p), number concentration (N), chemical composition, and hygroscopicity (Köhler, 1936; McFiggans et al., 2006; Reutter et al., 2009; Braga et al., 2021, Pöhlker et al., 2021). In the central Amazon and beyond, N and the PNSD are the primary factors defining the CCN concentration at a given water vapor supersaturation, whereas hygroscopicity and chemical composition are only of secondary importance (Dusek et al., 2006; Pöhlker et al., 2016; Pöhlker et al., 2018). The Amazonian submicron PNSD is characterized by a bi-modal shape during the wet season, comprising about equally strong Aitken and accumulation modes, with comparatively low concentration levels. In contrast to a monomodal shape during the dry season, comprising a strong accumulation and a largely covered/hidden Aitken mode, with comparatively high concentration levels (Zhou et al., 2002; Andreae et al., 2005; Pöhlker et al., 2016; Varanda Rizzo et al., 2018, Franco et al.,

https://doi.org/10.5194/egusphere-2023-1361
Preprint. Discussion started: 26 June 2023

2022). Particles between 10 and 50 nm are also detected at comparatively low concentrations, especially during the wet season when aerosol growth events are most pronounced (Franco et al., 2022). Machado et al. (2021) showed that the PNSDs at the Amazon Tall Tower Observatory (ATTO) are modulated by the degree of intensity of convective events, which increase the number concentration of sub-50 nm particles and decrease Aitken and accumulation mode particles, with different sensitivities when considering the two seasons and different measured heights.

Despite the strong efforts being made to understand and quantify aerosol properties, their effects have remained a major uncertainty in climate and Earth system models, which continuously motivates new studies and the development of novel techniques (Lee et al., 2016; Seinfeld et al., 2016; Fletcher et al., 2018; Forster et al., 2021). One approach for particles characterizations not much explored yet is the evaluation of microphysical processes in a 3D phase space. McFarquhar et al. (2015) performed the first-ever study using an N_0-λ-μ space based on the parameters of the gamma size distribution to characterize ice hydrometeors. They observed that an ellipsoid could describe the population of PNSDs studied, bounding the limits of the range of the parameters. The authors suggest that models could use this ellipsoid range as a parametrization scheme since it allows multiple relationships that are easily implemented in a stochastic framework. Improving this approach, Cecchini et al. (2017) took advantage of the same phase space, however, applying trajectories on it. They studied the evolution of cloud droplet size distributions in transitioning clouds from warm-phase microphysical properties to a mixed-phase layer, revealing the effects of what they defined as "pseudo-forces". These forces represent the physical processes causing the displacements in the space. Similarly, Hernandez Pardo et al. (2021) applied the same approach to study the variability of the spectral dispersion of droplet size distributions, proposing a parametrization for the shape parameter in bulk microphysics cloud-resolving models.

Essential data for aerosol studies in the Amazon and beyond is a robust knowledge of the total particle number concentrations and the PNSD (e.g., Guyon et al., 2003; Poschl et al., 2010; Andreae et al., 2015). These data are a full description of the multimodal PNSD and its variability in space (e.g., moving platforms) and time (e.g., long-term time series). For a detailed mechanistic understanding, however, the variability of the individual modes (i.e., sub-50 nm, Aitken, accumulation, and coarse modes) relative to each other is often relevant. As the modes typically have a significant extent of overlap, multi-modal lognormal fit functions are routinely applied to isolate the variability of isolated modes (e.g., Pöhlker et al., 2016; Varanda Rizzo et al., 2018; Franco et al., 2022). Here we use the multi-modal lognormal fitting based on a broad statistical basis to characterize and visualize the variability of the Amazonian submicron modes across seasons, diel patterns, and meteorological events. However, we go beyond traditional approaches by utilizing a novel interpretation technique that represents the PNSDs distribution in the N-D_g-σ phase space. This approach provides novel insights not only quantitatively, but also qualitatively and temporally, and has the potential to improve current aerosol parametrizations in Earth system models.

https://doi.org/10.5194/egusphere-2023-1361
Preprint. Discussion started: 26 June 2023

2 Data and Methods

This study makes use of the information of particle number size distributions (PNSDs) measured at the Amazon Tall Tower Observatory (ATTO) site, which is located in a pristine region of the Amazon rainforest, about 150 km to the northeast of Manaus (Andreae et al., 2015). The PNSD data were obtained by a Scanning Mobility Particle Sizer (SMPS) instrument, manufactured by TSI Inc, which is located inside a laboratory at the foot of the tower. The samples come from an inlet 60 m above the ground, which are corrected to standard temperature (273.15 K) and pressure (1013.25 hPa). The SMPS measurements cover a size range from 10 to 400 nm, with 104 bins, at a time resolution scan of 5 minutes. More information regarding the SMPS specifications can be found in Franco et al. (2022). The PNSD time series used in this study spans from May 2021 to April 2022, where the dry season spans from August to November, and the wet season from February to May. These definitions are based on aerosol-precipitation characterization, according to Pöhlker et al. (2016). A multi-modal lognormal fit was applied to each SMPS measurement by an algorithm specially optimized for ATTO region particles, as outlined in detail in Franco et al. (2022).

This study aims to characterize the PNSDs and also evaluate their interaction with precipitation. Therefore, a dataset of rain intensity (RI, in $mm.h^{-1}$) was used. The measurements were acquired by a disdrometer (Joss-Waldvogel, model RD 50, Distromet LTDA) located at the ATTO-Campina site, nearly 4 km from the ATTO tower site. This distance between the two sites is within the typical size of thunderstorms, around 25 km in diameter (Seeley & Rompos, 2015), therefore both sites are under the same environment. Machado et al. (2021) provide a full description of the ATTO-Campina site. The instrument measures the raindrop size distribution at the surface. It can distinguish 127 classes of drop diameter, whose output is given in 20 drop size classes. The RI data is given in a 5-minute resolution.

The methodology used in section 3.4 considered the moment of the maximum rain intensity that occurred per day, with a total of 87 days of valid data for the dry season and 86 days for the wet season. In section 3.5, the analyses considered afternoons, 13-18 Local Sidereal Time (LST) with and without precipitation. To capture a significant number of days for both cases, a threshold of 0.5 $mm.h^{-1}$ of rain intensity was applied. A rainfall afternoon event was defined as having at least one record higher than the threshold, while a no-rainfall event had all records below the threshold. During the dry season, 55 days were considered "without precipitation" and 31 days with precipitation, while in the wet season, there were 29 and 58 days, respectively. The morning aerosol background was based on these days, considering the values from 06 to 12 LST of each day.

2.1 Multi-modal lognormal fit

Conveniently used to represent a particle size distribution, the multi-modal lognormal fit describes the shape of an aerosol population by using three main parameters: the aerosol number concentration N (cm^{-3}), the mode geometric median diameter

https://doi.org/10.5194/egusphere-2023-1361
Preprint. Discussion started: 26 June 2023

D_g (nm) and the mode geometric standard deviation σ (nm). They are obtained by the application of the following Eq. (1) (Heintzenberg, 1994):

$$f(D_p, D_{gi}, N_i, \sigma_i) = \sum_{i=1}^{n=3} \frac{N_i}{\sqrt{2\pi}\ln(\sigma_i)} \times exp\left\{-\frac{[\ln(D_p)-\ln(D_{gi})]^2}{2ln^2(\sigma_i)}\right\} \quad (1)$$

where D_p is the particle diameter, and i is the number of aerosol size modes, according to the characteristic multi-modal Amazonian particle population (Pöhlker et al., 2016; Machado et al., 2021, Franco et al., 2022). The three modes and size ranges considered in this study are defined as sub-50 nm (10-50 nm), Aitken (50-100 nm), and accumulation (100-400 nm).

Each SMPS scan of the time series from May 2021 to April 2022 was fitted using Eq. (1), resulting in an output of the three parameters for each mode per each time scan. To avoid unrealistic fittings, only D_g that matched its respective mode size range was used. In addition, only R^2>0.9 for total number concentration was considered and an outlier filter considering the top 1% (Percentile 99) was applied to all parameters. The data processing resulted in a total of 57820 useful PNSDs.

With the parameters presented in the Results section, one can reproduce a PNSD curve by applying them in Eq. (1). In the present study, all analyses were done by computing the mean of each mode's parameters with respect to the temporal resolution used. The resulting PNSD curve emphasizes the three modes, as shown in Fig. S1.

2.2 The N-D_g-σ phase space

The representation of PNSDs in a 3D phase space enables the visualization of a permutation of possibilities. In an N-D_g-σ phase space, each parameter is orthogonal to the other, as shown in Fig. 1a. In this space, each data point corresponds to one fitted PNSD that can be interpreted as a curve describing the PNSD at a specific time. Figure 1a displays the N-D_g-σ space by dividing it into 8 sub-cubes with corresponding idealized PNSDs, to illustrate its interpretation. A trajectory in this space shows how the PNSD evolves in time. The present study considers the particle growth, the particle transport, the vertical movement, and the precipitation regimes as general pseudo-forces that modulate the displacements in the phase-space. Note that the orientation way of showing the space axes in the Results section was chosen to ease the plot's visualization, not always following the same orientation.

An example of a plot of the mean fit parameters representing the accumulation mode at ATTO for the dry and wet seasons is shown in Fig. 1b. It illustrates the trajectory of the seasonal back and forth between the two seasons' properties of the PNSDs, being bridged by sub-cubes 2 and 8 of Fig. 1a. This localization means that the dry-wet trajectory presents a decrease in N and σ and an increase in the D_g dimension. Since it is dealing with a seasonal trajectory, the precipitation regime, and the horizontal transports are the main pseudo-forces causing the displacement seen. Therefore, the accumulation mode goes from a high to a low number concentration, to a low to a high geometric diameter, and a broad to a narrow curve when going from the dry to the wet season. All these characteristics can be seen in Fig. 1c.

https://doi.org/10.5194/egusphere-2023-1361
Preprint. Discussion started: 26 June 2023

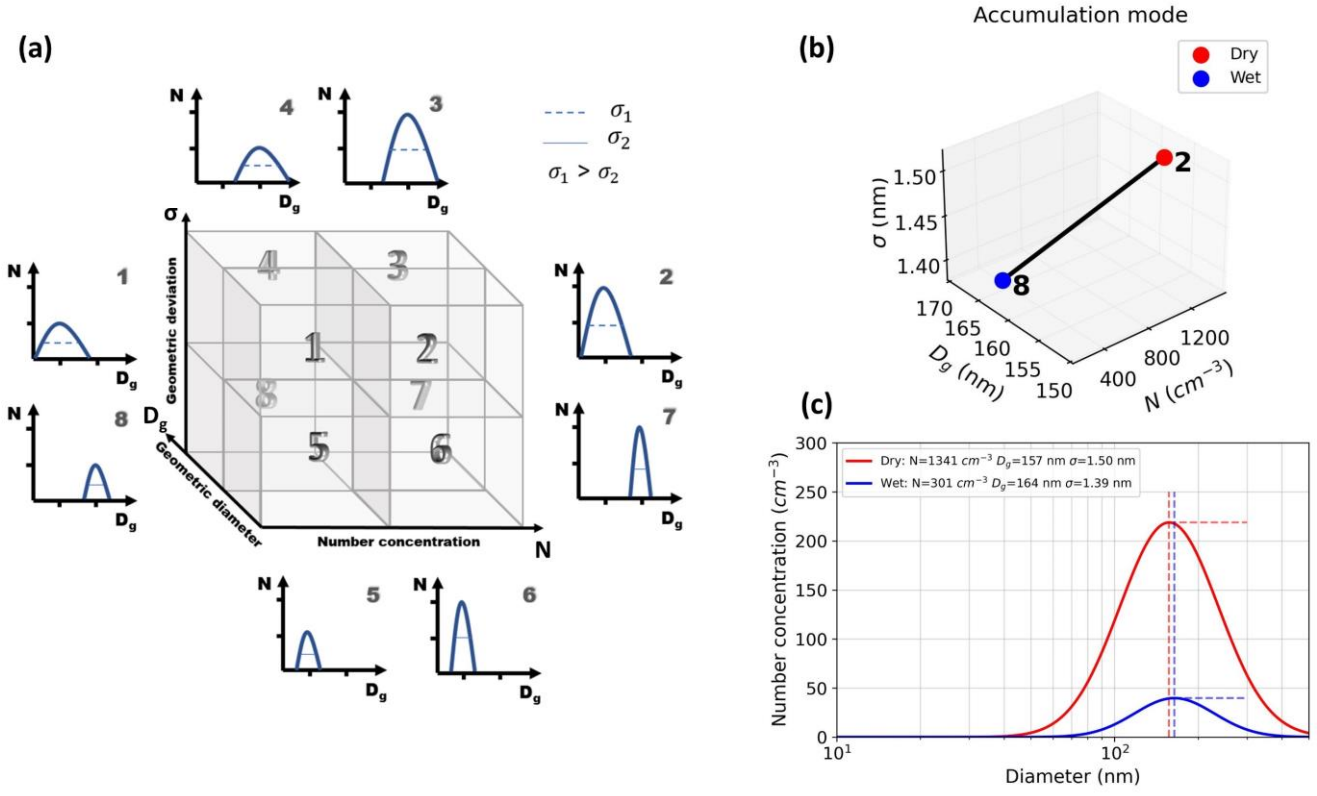

Figure 1. Conceptual drawing of the properties of the particle size distribution in the N-D_g-σ phase space. (a) Expected distributions when placed in specific areas of the phase space; (b) Trajectory from the dry to the wet season of the accumulation mode data used in this study. The numbers represent the location in the conceptual space; (c) The distribution of the curves using the computed mean parameters. As expected from the conceptual drawing going from sub-box 2 to 8, there is a decrease in the peak of number concentration, a displacement to a higher diameter, and a narrower curve. Source: Authors.

3 Results and Discussions

3.1 Characterization of the PNSDs

The analysis of Amazonian PNSDs by lognormal fits with the N-D_g-σ phase space, introduced in this study, reveals characteristic patterns and paths in this phase space. Based on a broad statistical basis of one year of measurements, the following results show the arrangement of all PNSDs in hourly resolution, colored by kernel density probability, where every data point represents a full PNSD.

The sub-50 nm distribution is known to have the most pronounced growth and relative concentration amplitude, especially in the wet season (Machado et al., 2021; Franco et al., 2022). By observing its configuration in the phase space (Figure 2a), one can notice a core at very small particles and very low concentration. This core comprehends PNSDs with $10 \leq D_g < 20$ nm and $0 < N \leq 20$ cm^{-3}, corresponding to 13.1% of the total distribution. It can be indicating a starting point of the mode, which is

https://doi.org/10.5194/egusphere-2023-1361
Preprint. Discussion started: 26 June 2023

dominated by sub-20 nm particles that can later proceed to grow into larger particles or that remain as small particles. This discussion continues in sections 3.2 and 3.3. It is worth commenting that the SMPS used is limited to 10 nm, thus the complete distribution of nucleation particles, those from a few nanometers to about 10 nm, is not measured. A more profound comprehension of this core could only be done by considering the contribution of these particles, measured with a Nano SMPS.
175 In general, the sub-50 nm spatial distribution shows a specific pattern, characterized by a curved cone volume.

Differently from the sub-50 nm, the Aitken PNSDs show a surface with nearly constant dispersion, with a variation in D_g and in N. They range from 70 to 90 nm, and from 100 to 300 cm^{-3}, respectively, consistent with Pöhlker et al. (2016) and Varanda Rizzo et al. (2018). This variation in both D_g and N can indicate that as the particles age and grow, which increases the dominant diameter of the distribution, there is a simultaneous change in concentration. This behavior will be later explored in
180 sections 3.2 and 3.3. The highest density core is centered at 200 cm^{-3} with D_g at 70 nm and σ at 1.2 nm (Figure 2b). In the ND_g axis surface, the data density decreases radially, which shows that the central distribution is representative of the whole PNSDs, including all seasons. While on the other axes, the distribution width is more axially flattened. This arrangement characterizes a 3D semi-sphere.

Dominated basically by N, the accumulation mode PNSDs are distributed in a geometric figure that resembles a cylinder
185 (Figure 2c). This volume has a small range in D_g and σ, and an extended range in N. This feature emphasizes the seasonal cycle of the accumulation mode, which has higher concentrations in the dry season and lower ones in the wet season, associated with smaller changes in the D_g and inσ. The highest density is observed at the bottom of the cylinder, in the area of comparatively low N, and D_g between 150 and 200 nm.

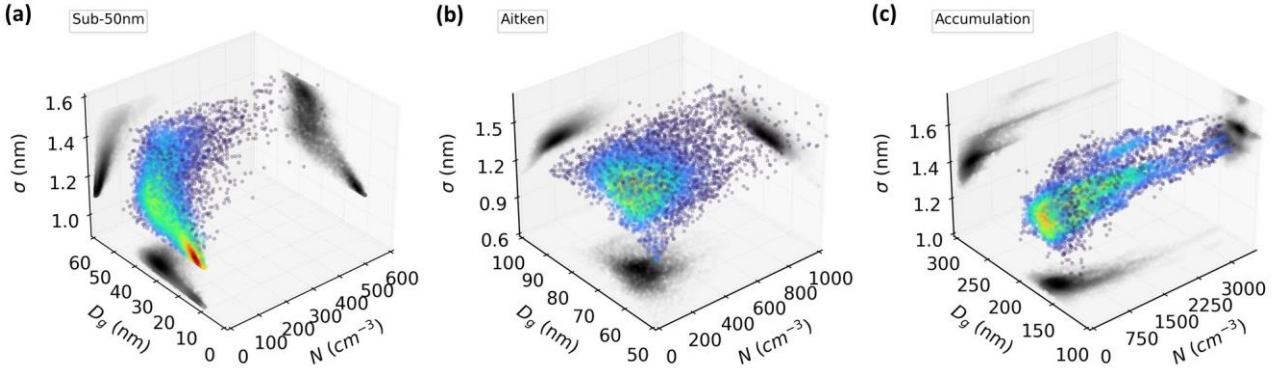

190 **Figure 2. Hourly Amazonian PNSDs arrangements in the N-D_g-σ phase space. The patterns show the distribution of the (a) sub-50 nm, (b) Aitken, and (c) accumulation modes. Every data point represents one full PNSD. In color is the density of the data points, with respective projections in grey scale shadows on all three axes. The distribution considered spans one year of measurements (May 2021 to April 2022).**

https://doi.org/10.5194/egusphere-2023-1361
Preprint. Discussion started: 26 June 2023

3.2 Seasonal trajectories

Trajectories in the N-D_g-σ phase space allow the visualization of the displacements between PNSDs, showing the variability causes due to the existing pseudo-forces. The following results show the seasonal characteristics and reveal a monthly path in the phase space. The specific distribution of each parameter per month can be seen in Fig. S2.

The accumulation mode trajectory resembles an ellipse in all three projections (Figure 3c), influenced mainly by N and, to a minor extent, by D_g. From December-January, the seasonal cycle presents the highest D_g, around 175 nm, while the other parameters are lower when compared to the whole trajectory (σ=1.4 nm, N=500 cm^{-3}). In the wet season, the trajectory is basically changed by a decrease in D_g, to ~164 nm. This trend goes until an inflection point in August-September, with N of ~1800 cm^{-3}, σ of 1.5 nm, and D_g of 154 nm. This particular period marks the beginning of the dry and polluted season. The relatively high aerosol number concentration is influenced by the transition from the wet to the dry season, which starts to be characterized by a more polluted atmosphere, dominated especially by anthropogenic biomass burning (Andreae et al., 2015; Pöhlker et al., 2018). From this point on, the trajectory returns to the beginning state, with the wet season characteristics. The mean season's parameters can be found in Fig. 1c, which shows an opposite behavior regarding N and D_g.

The dry season for the accumulation mode is characterized by high N, but small D_g, whilst the wet season presents low N, but bigger D_g. This pattern is likely due to the different sources of aerosols, from the predominance of mostly anthropogenic nearby fires in the dry season to aged long-range-transport, like African dust and Atlantic marine aerosols, in the wet season (Pöhlker et al., 2018; Holanda et al., 2020). The trajectory revealed that the transition months, December-January and June-July, present the highest and lowest D_g, respectively. Also, the last two months of each season, April-May and September-October, are characterized by nearly the same D_g, but with different N and curve width (σ).

The Aitken mode trajectory (Figure 3b) shows that its seasonal transition also follows the same behavior observed in the accumulation mode trajectory, presenting the extremes in D_g, 74 nm (DJ) and 67 nm (JJ). Following Pöhlker et al. (2018), during biomass burning in the dry season, the accumulation mode dominates the Aitken mode regarding N, while during the wet season, which has a near pristine environment, the Aitken mode is more equivalent (also seen on Fig S1). From Fig 3b, the effects of this oscillation are perceived. The wet season (N~290 cm^{-3}, σ~1.31 nm, D_g~69 nm) is characterized by an approximately constant D_g and σ, a function of basically N. On the other hand, the dry season (N~300 cm^{-3}, σ~1.30 nm, D_g~70 nm) is characterized by nearly constant N, increasing in D_g. This behavior can elucidate the circular pattern seen in the ND_g axis surface in Fig. 2b.

The sub-50 nm mode monthly trajectory (Figure 3a) is limited to a D_g range between ~26 and ~32 nm, nearly the same gap between the two density cores seen in the ND_g axis surface in Fig. 2a. Although the core of smaller PNSDs contributes to only 13.1%, the two points in Fig. 3a, representing the wet season, FM and AM, are the ones with a shift to smaller D_g. It is indeed during the wet season that most of these sub-20 nm PNSDs are happening, as seen in Fig. S3a, representing about 20% of all

https://doi.org/10.5194/egusphere-2023-1361
Preprint. Discussion started: 26 June 2023

PNSDs. New particle formation has been reported to happen mostly in this season, associated with rainfall events (Wang et al., 2016; Andreae et al., 2018; Franco et al., 2022). Therefore, the core seen can be related to distributions capturing the "birth" of these particles.

A notable behavior is that sub-50 nm PNSDs in both wet and dry seasons show the same N, changing the D_g of the distribution. The dry season is characterized by D_g =30 nm, while the wet season has D_g ~27 nm. The sub-50 nm PNSDs seem to be most affected by the transition regimes, presenting the two extremes in N. The peak observed in JJ, the period of clean to polluted transition, is shifted to larger particles, where a major part of the second core in larger particles and higher concentration (Figure 2a) could be associated with this period.

By analyzing the three modes' trajectories, all of them presented extremes either in N or D_g in transition months. This feature is likely related to the effect of rainfall regimes on size distribution, since sub-50 nm increases its concentration, and Aitken and accumulation modes decrease during rainfall events (Machado et al., 2021).

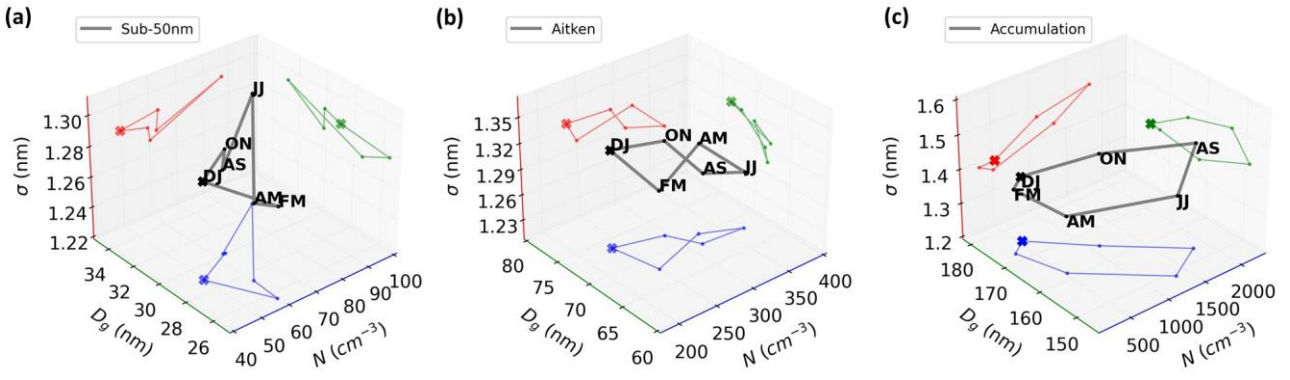

Figure 3. Seasonal trajectories of Amazonian PNSDs in the N-D_g-σ phase space. The trajectory is shown in bimonthly resolution, showing the patterns of the (a) sub-50 nm, (b) Aitken, and (c) accumulation modes. The cross symbol marks a visual reference and the colored trajectories are projections in each axis surface.

3.3 Diurnal cycle trajectories

Machado et al. (2021) showed that the diurnal cycle number concentration of the three aerosol modes is well-defined. The authors revealed that sub-50 nm mode N is strongly controlled by the diurnal cycle, reaching a maximum during the night probably due to late afternoon rainfalls, and reaching a minimum as the sun rises when particle growth initiates, which is also corroborated and described by Franco et al. (2022). Aitken and accumulation modes follow an opposite behavior, increasing in N with the sunrise reaching a maximum in nearly the middle of the afternoon, starting to decrease due to dry deposition and scavenging, until achieving a minimum during the night and early morning. The following results (Figure 4) confirmed this cycle and unfolded the link to diameter change. To show the diurnal cycle trajectories more clearly, the times were plotted by every 6 LST.

https://doi.org/10.5194/egusphere-2023-1361
Preprint. Discussion started: 26 June 2023

The sub-50 nm mode diurnal cycle in the dry season (Figure 4a) shows a strong link to all three parameters. The trajectory changes linearly from midnight to noon, and vice-versa. The concentration decreases until the minimum at 12 LST and increases until the maximum at 00 LST. The D_g and σ also follow this pattern, with the minimum D_g of about 28 nm and the maximum of about 32 nm. When the sun rises (06 LST), particle growth starts to dominate, given that N and D_g decrease. The primary distinction between the dry and the wet seasons lies in the range of D_g observed. Specifically, during the wet season, the diameter amplitude tends to be lower, which can be attributable to the prevalence of sub-50 nm rapidly growing into Aitken particles and/or by distributions without growth. Conversely, during the dry season, the advection of particles may contribute to the greater variability in the diameter of the particle size distribution. The second core seen in larger sub-50 nm PNSDs (Figure 2a), could be partly associated with diurnal features of the dry season.

Franco et al. (2022) pointed out a value of 88% of growth events of sub-50 nm associated with new particle formation to happen in the wet season. The diurnal trend specifically for these cases showed a peak in concentration in the early morning, which could explain the peak seen in Fig 4d at 06 LST. Comparing with Fig. 2a, where a core around 20 nm is observed, the diurnal cycle does not show average diameters around this value. This could be associated either with the low frequency of occurrence of these sub-20 nm PNSDs (only 13.1%) or because of being equally distributed throughout the day. Figure S3b elucidates this fact by revealing that there is actually a diurnal pattern, but indeed happening at a low frequency. This diurnal cycle reinforces that these sub-20 nm PNSDs are produced by rainfall events since the pattern seen resembles a rainfall diurnal cycle, that mainly happens in the afternoon, but also shows a peak in the morning.

The diurnal cycle for the Aitken mode is different among the seasons. In the wet season (Figure 4e), the whole cycle occurs at nearly constant N, with a change in the D_g and σ, that decreases from 00 to 12 LST with a following increase from 12 to 18 LST. The concentration stability could be explained by a balance between the aerosol growth events from the sub-50 nm to the Aitken mode and from the Aitken to the accumulation. In contrast, the changes in diameter are dominated first by growth events from the sub-50 nm to the Aitken mode in the morning (06-12 LST) and second by growth from the Aitken to the accumulation mode in the afternoon (12-18 LST). This behavior coincides with the decrease in N and the increase in D_g from 06-12 LST in the sub-50 nm cycle (Figure 4d), and with the D_g growth in the accumulation mode cycle (Figure 4f) from 12-18 LST. In other words, in the morning, it seems to have no other source of Aitken particles than the growing process from sub-50 nm. In the afternoon, Varanda Rizzo et al. (2018) showed that there is a source of Aitken mode associated with the transport by downdrafts into the boundary layer, although it can also act as a sink due to the association with precipitation. This source from downdrafts could explain the stability in N during the afternoon.

These findings conclude the comprehension of the core in sub-20 nm (Figure 2a): a substantial contribution for the density is of a prevalence of sub-20 nm PNSDs that remain with small particles, occurring in the afternoon, and a minor contribution is of sub-20 nm PNSDs that rapidly grow into Aitken, happening in the morning.

https://doi.org/10.5194/egusphere-2023-1361
Preprint. Discussion started: 26 June 2023

For the dry season, the Aitken mode diurnal cycle evolution (Figure 4b) is different from the wet season, and the main variation is at the particle number concentration (N). During the night and early morning, the particles are confined inside the nocturnal boundary layer and reach the maximum concentration. During the day, with the development of the boundary layer, the aerosol number concentration is reduced, and their size increases, also showing a growing process to accumulation mode. Unlike the wet season, in the dry season, the growth rate from Aitken to accumulation mode seems to be faster and the most predominant process rather than the growth from sub-50 nm to Aitken, resulting in a decrease in the Aitken number concentration during the growing process. This is in accordance with Franco et al. (2022), who showed that only 12% of sub-50 nm growth events happen during the dry season.

The accumulation mode in the dry and wet seasons (Figures 4c and 4f) have nearly the same pattern, only shifting in N and in D_g according to the season's features. Note that the axes are rotated, and disposed differently of from the others to improve the visualization. The cycle is characterized by a minimum in both N and D_g at 06 LST, followed by an increase until 12 LST, corresponding to the time when the Aitken mode is reduced, and a following decrease until back to sunrise (06 LST), probably associated with the afternoon rainfall and the scavenging processes. D_g variation goes from around 155 nm to 158 nm in the dry, and from about 162 nm to 165 nm in the wet season. The minimum and maximum concentration match with the sink and growth process of the day (06 and 12 LST), respectively.

https://doi.org/10.5194/egusphere-2023-1361
Preprint. Discussion started: 26 June 2023

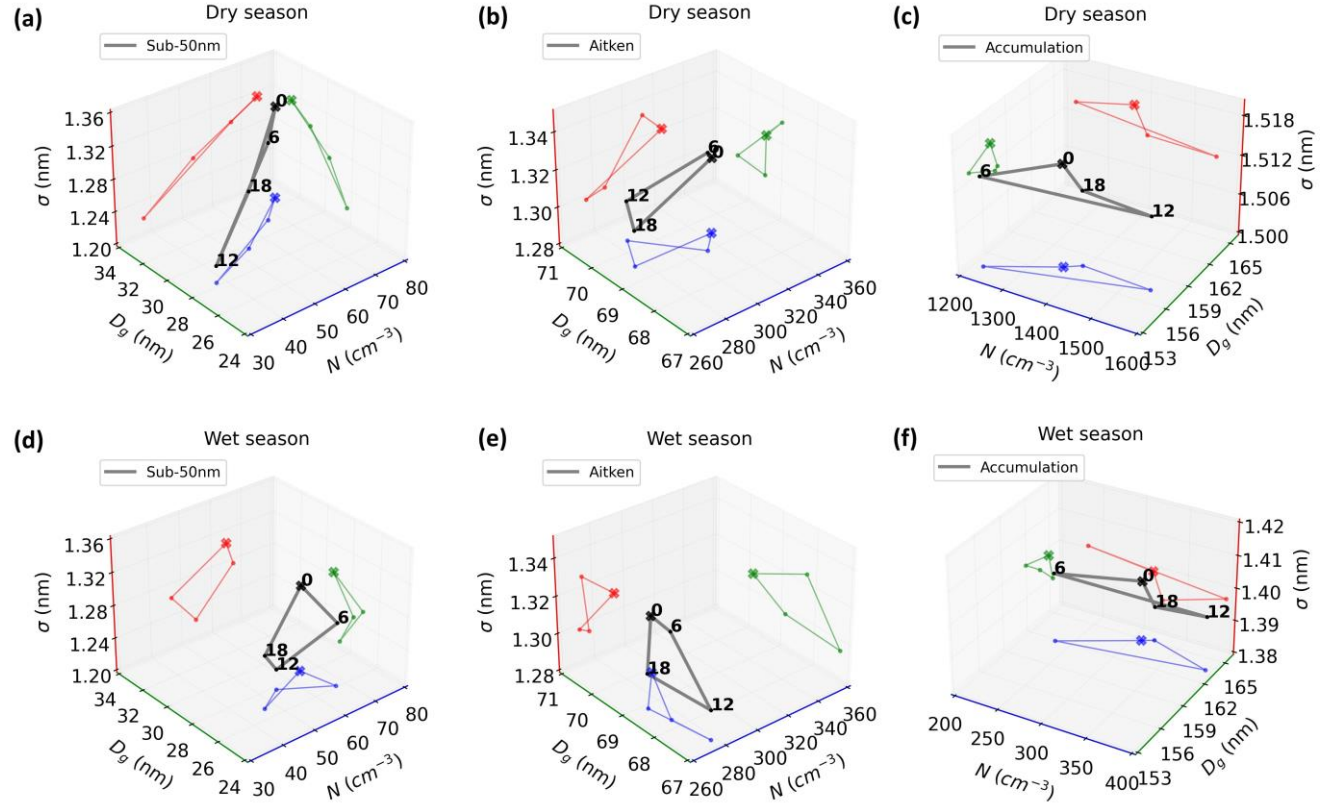

Figure 4. Diurnal cycle trajectories of Amazonian PNSDs in the N-D_g-σ phase. The trajectories show the patterns of each mode (columns) for each season (rows). The numbers in black represent the time in LST, the cross symbol marks a visual reference, and the colored trajectories are projections on each axis surface. The cubes (c) and (f) are slightly turned to better visualize the trajectories.

3.4 Effects of precipitation on PNSD

Machado et al. (2021) studied the relationship between lightning and PNSD and found out that the Aitken and the accumulation modes concentration decrease at the same time sub-50 nm mode increases with the maximum intensity of lightning. This behavior begins to occur 100 minutes before the maximum lightning density, indicating this moment as the beginning of the rainfalls, which match its maximum with maximum lightning density. This finding characterizes the course of the particles regarding their number concentration. Since lightning and precipitation peak simultaneously (Mattos et al., 2017) the following results (Figure 5) are intercomparable, promoting a complete characterization of the aerosol-precipitation interaction. Note that for better visualization, the accumulation mode axes are rotated (the same configuration that was presented in Figures 4c and 4f).

In the dry season, sub-50 nm (Figure 5a) N keeps constant at around 60 cm^{-3} increasing only the dominant D_g also at constant σ, until maximum precipitation. From the precipitation peak, the PNSDs start to increase in D_g after 1-2 hours and reach the

https://doi.org/10.5194/egusphere-2023-1361
Preprint. Discussion started: 26 June 2023

highest N 3 hours later. In the wet season (Figure 5d), the post-maximum increase in N and D_g is also seen, although the maximum occurs 2 hours later. It is at 2 hours before and after that the two extremes in D_g occur, reaching the minimum and maximum, respectively. This might be related to the start and end of the precipitation event, nearly the same moments seen by Machado et al. (2021). This feature is more sensible in the wet than in the dry season.

Many studies have been reporting that in the wet season, sub-50 nm particles increase in concentration after a precipitation event (Wang et al., 2016; Andreae et al., 2018; Franco et al., 2022). The results here confirm this increase, also observing the same behavior in the dry season, although with a lower increase. In addition, it was shown a parallel increase in diameter.

Larger particles are washed out by precipitation, therefore, a decrease in concentration is expected. In fact, this can be seen for the Aitken and the accumulation modes. However, the results revealed that they are also characterized by bigger and smaller particles, before and after the maximum, respectively. This diameter change is more significant in the wet season, possibly due to the higher accumulated precipitation in this season (Machado et al., 2004).

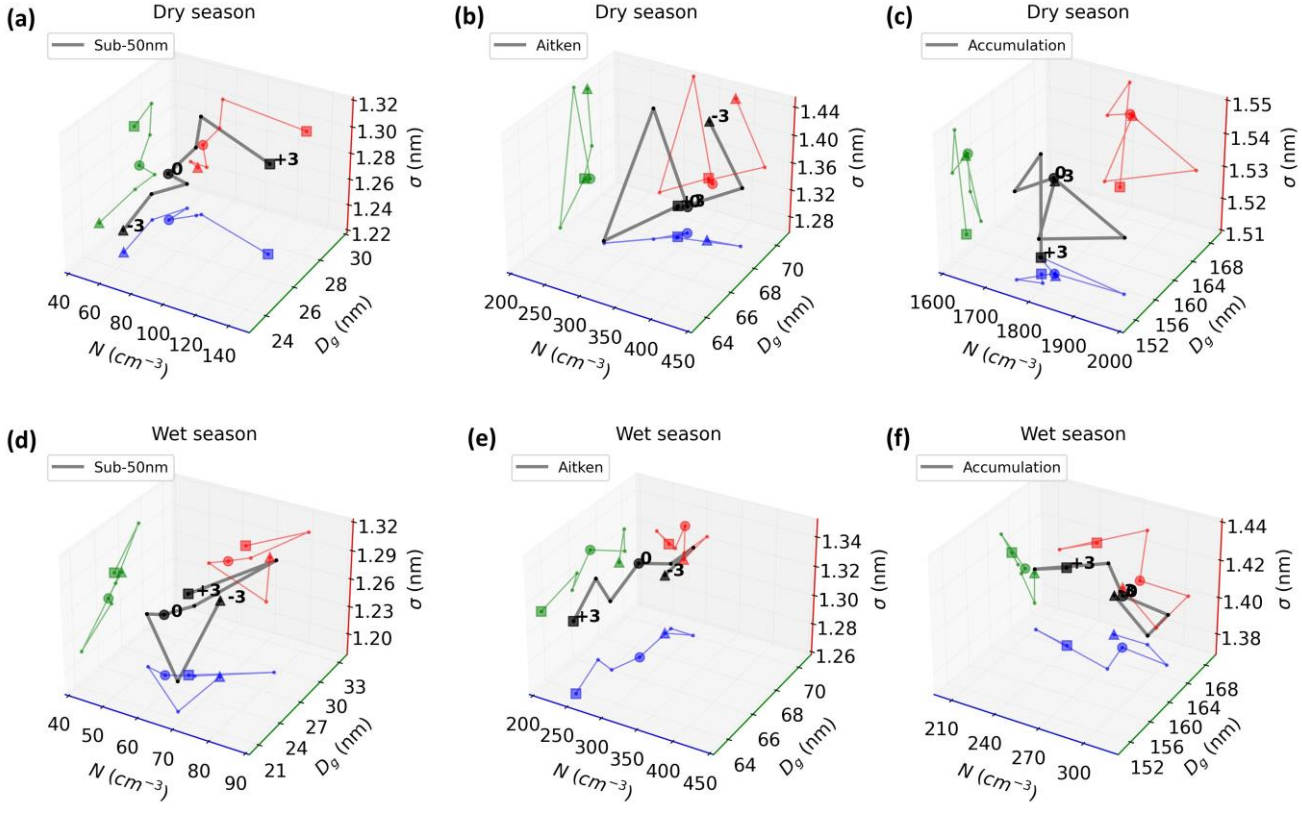

Figure 5. Composites of Amazonian PNSDs in the N-D_g-σ phase space for before and after maximum precipitation. The trajectories span from 3 hours before (triangular symbol) to 3 hours later (square symbol), considering the moment of maximum precipitation (circle symbol), for each mode (columns) and each season (rows).

https://doi.org/10.5194/egusphere-2023-1361
Preprint. Discussion started: 26 June 2023

3.5 Trends in the accumulation mode PNSDs trajectories when associated with precipitation occurrence

The following analysis explored the morning background trajectories considering afternoons with and without precipitation. The aerosol mode that has the most influence on precipitation, acting as CCN, is the accumulation mode. Initially, the analysis was performed for all three modes, however, the sub-50 nm mode did not exhibit any difference in the early morning trajectories (not shown). The Aitken mode slightly displayed some differences (not shown), but effectively, the accumulation mode was the one that clearly showed different patterns. Therefore, the following analysis of Figure 6 was done exclusively for this mode, which exhibited clear preferential characteristics and trajectories in the phase space.

In the dry season (Figure 6a), the early morning trajectories of both cases show an increase in concentration, characterized by the diurnal cycle, at different rates though. Days with precipitation in the afternoon are preceded by noons with lower concentrations. In the dry season, the Amazonian PNSD is monomodal, dominated by the accumulation mode with a large concentration (Figure S1). Nevertheless, aerosol concentration is so high that the amount of these particles needed for CCN activation seems to no longer be a causal factor. In contrast, bigger particles, which increase the dominant D_g of the PNSDs, seem to be present in the mornings with precipitation in the afternoon. In the dry season, the diameter of the aerosols appears to have the most influence on precipitation to occur, rather than the concentration.

For the wet season (Figure 6b), the accumulation mode shows the same general pattern as in the dry season. It presents the same concentration trajectory for both cases, with a shift to larger particles in rainfall cases, but with a concentration trajectory that goes further. This shows that due to the lower number concentration in the wet season, both concentration and diameter have an equal influence on precipitation. Machado et. al (2021) showed that in the wet season, a high accumulation mode concentration background is associated with a maximum activity of lightning events 150 min later, possibly indicating an invigoration of convective clouds. Based on Fig. 6b, it seems that this high-concentration background is also ruled by larger accumulation particles.

In general, rainy days have shown a D_g in the morning increased by ~10 nm compared to days without precipitation. This same feature is also present in Fig 5, confirming that precipitation events are preceded by larger accumulation particles. Hernández Pardo et al. (2021) showed that Amazon clouds in a more polluted environment presented a smaller variability in droplet size distribution width due to CCN being already large enough to produce droplets. This large size seen in the morning seems to be associated with the factors that can promote precipitation in the afternoon, of course probably along with other favorable conditions, such as high humidity. The observed features highlight the importance in considering in aerosol parameterization not only the total particle concentration, but also the aerosol-size distribution.

https://doi.org/10.5194/egusphere-2023-1361
Preprint. Discussion started: 26 June 2023

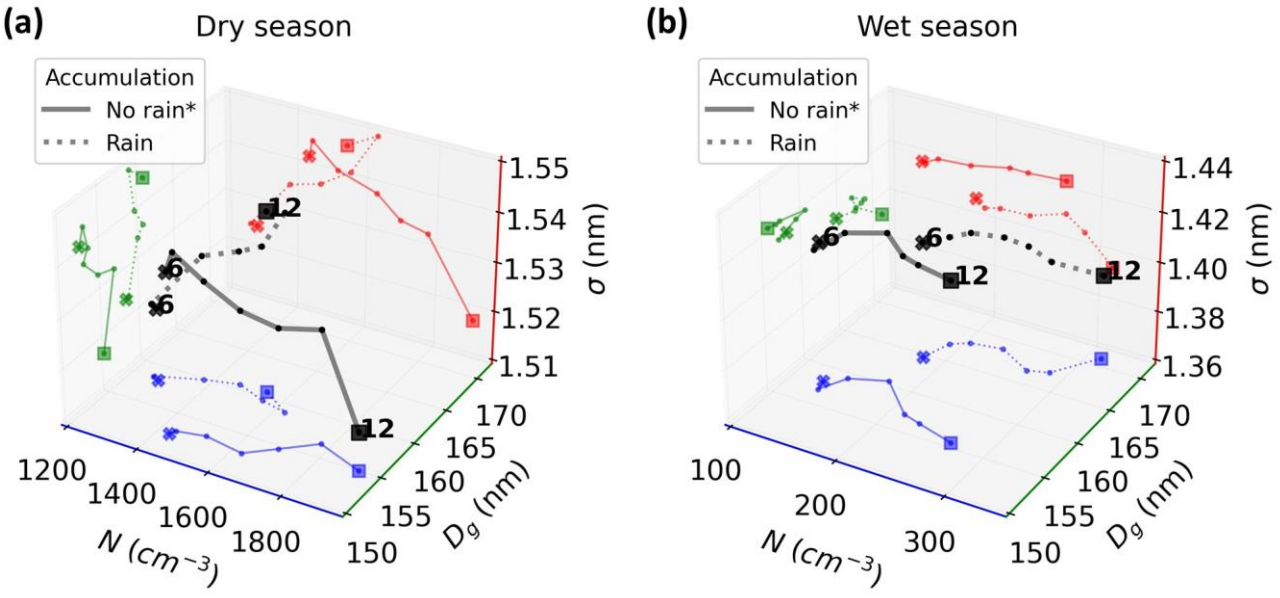

Figure 6. Composites of Amazonian PNSDs in the N-D_g-σ phase space for days with and without precipitation. The trajectories are in the morning, going from 6 (cross marker) to 12 (square marker) LST, for cases of afternoons with and without rainfall events. An afternoon with rainfall was defined as having at least one record of rain intensity (RI) ≥ 0.5 mm.h^{-1} from 13 to 18 LST, while a no rainfall afternoon was defined as having all records of RI < 0.5 mm.h^{-1}.

4 Summary and conclusions

Amazonian particle number size distributions (PNSDs) were analysed by implementing a new approach, the N-D_g-σ phase space, a 3D space based on the fit parameters of a multi-modal lognormal function. The parameters are the number concentration (N), the geometric median diameter (D_g), and the geometric deviation (σ). The fit was applied to in situ SMPS data covering 1 year, measured at the ATTO tower, in central Amazonia. Visualizing the arrangements of each PNSD mode in the phase space enabled a volumetric characterization of a population of PNSDs and a time evolution analysis by trajectories.

In the phase space, the sub-50 nm PNSD population was represented by a curved cone volume, the Aitken PNSDs by a semi-sphere, and the accumulation PNSDs by a cylinder. This is the first glance of the volumetric characterization of Amazonian aerosol modes distributions. The knowledge of such volumes bounds the limits of these distributions, elucidating all possible solutions of a PNSD, providing the tools for parameterization development.

The seasonal trajectory of the accumulation mode PNSDs in the N-D_g-σ has a well-defined cycle, characterized by an ellipsoid. The extremes in D_g values occur during the transition months, December-January and June-July, presenting the highest and lowest values, respectively. The fit parameters for the dry season were N=1368 cm^{-3}, D_g=157 nm, and σ=1.50 nm, while for the wet season N=285 cm^{-3}, D_g=164 nm, and σ=1.39 nm. The Aitken mode PNSDs in the wet season are characterized by an approximately constant diameter (D_g~69 nm) and deviation (σ~1.31 nm), being a function of basically N, while in the dry

https://doi.org/10.5194/egusphere-2023-1361
Preprint. Discussion started: 26 June 2023

season, it is characterized by nearly constant concentrations (N~300 cm^{-3}), increasing in diameter. The seasonal trajectory of the sub-50 nm mode PNSDs presented a similar number concentration (N=60 cm^{-3}) in both dry and wet seasons, changing the diameter, D_g=30 nm, and D_g~27 nm, respectively.

The diurnal cycle during the dry season of the PNSDs of sub-50 nm mode follows a linear trajectory with a positive slope in all three axes, which is dependent on all three parameters. The trajectory decreases (increases) in all three parameters from 00 to 12 LST (12 to 00 LST). In the wet season, the cycle shrinks, and there is less variation in the D_g. The Aitken mode PNSDs diurnal cycle has different patterns when comparing the two seasons, characterized by a nearly constant N in the wet season. In contrast, in the dry season, it is the diameter that keeps constant. This behavior in the wet season can be explained by an equilibrium in concentration gain and loss due to the growing process from the sub-50 nm to the Aitken mode and from the Aitken to the accumulation mode. Regarding the changes in diameter, the first process dominates in the morning and the second in the afternoon. This feature indicates no other source of Aitken mode particles in the morning than the growing process from sub-50 nm. In the dry season, the growth from the Aitken to the accumulation mode dominates, promoting a decrease in N. For the accumulation mode PNSDs, the diurnal cycle seems to depend on N, with few variations in D_g and σ, in both seasons. The cycle's extremes in N are at 06 LST (minimum) and 12 LST (maximum), matching with sink and growth processes that occur during the day.

A density core in sub-20 nm PNSDs was observed in the arrangements of all sub-50 nm PNSDs, representing 13.1%. This core was associated with a substantial occurrence of these PNSDs during the wet season, especially from PNSDs remaining as sub-20 nm, happening during the afternoon. A minor occurrence of these sub-20 nm PNSDs was associated with a rapidly growing process to the Aitken mode, which happens in the morning. The cause of this pattern showed to be linked to the diurnal cycle of precipitation, possibly associated with new particle formation. Future studies should focus on investigating sub-10 nm particles and their contribution to the particle growing process.

Finally, the two-way effect of precipitation and PNSDs was explored. After maximum rain intensity, sub-50 nm PNSDs not only increase in N but also in D_g. This increase starts after 1 hour, going up to 2 hours after the rain peak, suggesting that this effect is due to new particle formation or sub-10 nm particle growth. At the beginning of the precipitation events, sub-50 nm PNSDs reach a minimum in D_g. For Aitken and accumulation mode, a decrease in N and D_g was seen after maximum precipitation, and before the maximum, N and D_g were higher. By analyzing how accumulation mode PNSDs background trajectories in the morning would affect the precipitation during the afternoon, we concluded that how big the accumulation particles are can be associated with the possibility of precipitation to occur. Days with afternoon precipitation had early morning accumulation mode particles larger than days without precipitation. The D_g is increased by ~10 nm. The trajectory revealed that for both cases there is an increase in N from 06 to 12 LST, however, it is only in the wet season that both N and D_g seem to be one of the factors for precipitation to occur. While in the dry season, it is exclusively the D_g, as the particle

https://doi.org/10.5194/egusphere-2023-1361
Preprint. Discussion started: 26 June 2023

concentration background in the dry season is already very high, larger than 1000 cm^{-3}. Further investigations must be done linking this diameter effect with thermodynamical conditions.

This study provided an overview of Amazonian PNSDs variability in the N-D_g-σ phase space and its trajectories, which facilitated the physical interpretation of processes involving particle source, sink, and growth, and elucidated possible aerosol-cloud parameterizations.

Author contributions

GRU and LATM designed the study. GRU processed the data. GRU, LATM and CP wrote the manuscript. MAF, PA, UP, LK and MLP provided valuable ideas for the data analysis and the interpretation of the results. LATM and CP supervised the study. All authors revised the manuscript.

Acknowledgments

We would like to thank the finantial support done by the São Paulo Research Foundation (FAPESP), by the Coordenação de Aperfeiçoamento de Pessoal de Nível Superior - Brasil (CAPES), by the Bundesministerium für Bildung und Forschung, by the Brazilian Ministério da Ciência, Tecnologia e Inovação, and by the Max Planck Society. For the operation of the ATTO site, we acknowledge the support of the Instituto Nacional de Pesquisas da Amazônia (INPA), the Amazon State University (UEA), the Large-Scale Biosphere-Atmosphere Experiment (LBA), FAPEAM, the Reserva de Desenvolvimento Sustentável do Uatumã (SDS/CEUC/RDS-Uatumã), and the Max Planck Society. Particularly, we would like to thank the ATTO-Campina team involved in the technical, logistical, and scientific support.

Finantial support

This research has been supported by the São Paulo Research Foundation (FAPESP), grants #2021/03547-7, #2022/01780-9, and #2022/07974-0, by the Coordenação de Aperfeiçoamento de Pessoal de Nível Superior - Brasil (CAPES) - Finance Code 001, by the Bundesministerium für Bildung und Forschung (BMBF contracts 01LB1001A, 01LK1602B, and 01LK2101B), by the Brazilian Ministério da Ciência, Tecnologia e Inovação (MCTI/FINEP contract 01.11.01248.00) and by the Max Planck Society.

References

Albrecht, B.A.: Aerosols, Cloud Microphysics, and Fractional Cloudiness, Science, 245, 1227–1230, https://science.sciencemag.org/content/245/4923/1227, 1989.

https://doi.org/10.5194/egusphere-2023-1361
Preprint. Discussion started: 26 June 2023

Aitchison, J., and Brown, J. A. C.: The Lognormal Distribution Function, Cambridge Univ. Press, London, UK, http://www.statlit.org/pdf/1957-Aitchison-Brown-Excerpts.pdf, 1957.

Andreae, M. O., Acevedo, O. C., Araújo, A., Artaxo, P., Barbosa, C. G. G., Barbosa, H. M. J., Brito, J., Carbone, S., Chi, X., Cintra, B. B. L., da Silva, N. F., Dias, N. L., Dias-Júnior, C. Q., Ditas, F.Ditz, R., Godoi, A. F. L., Godoi, R. H. M., Heimann, M., Hoffmann, T., Kesselmeier, J., Könemann, T., Krüger, M. L., Lavric, J. V., Manzi, A. O., Lopes, A. P., Martins, D. L., Mikhailov, E. F., Moran-Zuloaga, D., Nelson, B. W., Nölscher, A. C., Santos Nogueira, D., Piedade, M. T. F., Pöhlker, C., Pöschl, U., Quesada, C. A., Rizzo, L. V., Ro, C.-U., Ruckteschler, N., Sá, L. D. A., de Oliveira Sá, M., Sales, C. B., dos Santos, R. M. N., Saturno, J., Schöngart, J., Sörgel, M., de Souza, C. M., de Souza, R. A. F., Su, H., Targhetta, N., Tóta, J., Trebs, I., Trumbore, S., van Eijck, A., Walter, D., Wang, Z., Weber, B., Williams, J., Winderlich, J., Wittmann, F., Wolff, S., and Yáñez-Serrano, A. M.: The Amazon Tall Tower Observatory (ATTO): overview of pilot measurements on ecosystem ecology, meteorology, trace gases, and aerosols, Atmos. Chem. Phys., 15, 10723–10776 https://doi.org/10.5194/acp-15-10723-2015, 2015.

Braga, R. C., Rosenfeld, D., Krüger, O. O., Ervens, B., Holanda, B. A., Wendisch, M., Krisna, T., Pöschl, U., Andreae, M. O., Voigt, C., and Pöhlker, M. L.: Linear relationship between effective radius and precipitation water content near the top of convective clouds: measurement results from ACRIDICON–CHUVA campaign, Atmos. Chem. Phys., 21, 14079–14088, https://doi.org/10.5194/acp-21-14079-2021, 2021.

Cecchini, M. A., Machado, L. A. T., Wendisch, M., Costa, A., Krämer, M., Andreae, M. O., Afchine, A., Albrecht, R. I., Artaxo, P., Borrmann, S., Fütterer, D., Klimach, T., Mahnke, C., Martin, S. T., Minikin, A., Molleker, S., Pardo, L. H., Pöhlker, C., Pöhlker, M. L., Pöschl, U., Rosenfeld, D., and Weinzierl, B.: Illustration of microphysical processes in Amazonian deep convective clouds in the gamma phase space: introduction and potential applications, Atmos. Chem. Phys., 17, 14727–14746, https://doi.org/10.5194/acp-17-14727-2017, 2017.

Dusek, U., Frank, G.P., Hildebrandt, L., Curtius, J., Schneider, J., Walter, S., Chand, D., Drewnick, F., Hings, S., Jung, D., Borrmann, S., and Andreae, M. O.: Size matters more than chemistry for cloud-nucleating ability of aerosol particles. Science, 312, 1375-1378, https://www.science.org/doi/10.1126/science.1125261, 2006.

Fernandes, K., Giannini, A., Verchot, L., Baethgen, W., and Pinedo-Vasquez, M.: Decadal covariability of Atlantic SSTs and western Amazon dry-season hydroclimate in observations and CMIP5 simulations, Geophys. Res. Lett., 42, 6793–6801, https://doi.org/10.1002/2015GL063911, 2015.

Fletcher, C. G., Kravitz, B., and Badawy, B.: Quantifying uncertainty from aerosol and atmospheric parameters and their impact on climate sensitivity, Atmos. Chem. Phys., 18, 17529–17543, https://doi.org/10.5194/acp-18-17529-2018, 2018.

Forster, P., Storelvmo, T., Armour, K., Collins, W., Dufresne, J. L., Frame, D., Lunt, D. J., Mauritsen, T., Palmer, M. D., Watanabe, M., Wild, M., and Zhang, H.: The Earth's energy budget, climate feedbacks, and climate sensitivity, in: Climate Change 2021: The Physical Science Basis, Contribution of Working Group I to the Sixth Assessment Report of the Intergovernmental Panel on Climate Change [Masson-Delmotte, V., P. Zhai, A. Pirani, S.L. Connors, C. Péan, S. Berger, N. Caud, Y. Chen, L. Goldfarb, M.I. Gomis, M. Huang, K. Leitzell, E. Lonnoy, J.B.R. Matthews, T.K. Maycock, T. Waterfield,

https://doi.org/10.5194/egusphere-2023-1361
Preprint. Discussion started: 26 June 2023

O. Yelekçi, R. Yu, and B. Zhou (eds.)], Cambridge University Press, Cambridge, United Kingdom and New York, NY, USA, 923–1054, doi:10.1017/9781009157896.009, 2021.

Franco, M. A., Ditas, F., Kremper, L. A., Machado, L. A. T., Andreae, M. O., Araújo, A., Barbosa, H. M. J., de Brito, J. F., Carbone, S., Holanda, B. A., Morais, F. G., Nascimento, J. P., Pöhlker, M. L., Rizzo, L. V., Sá, M., Saturno, J., Walter, D., Wolff, S., Pöschl, U., Artaxo, P., and Pöhlker, C.: Occurrence and growth of sub-50 nm aerosol particles in the Amazonian boundary layer, Atmos. Chem. Phys., 22, 3469–3492, https://doi.org/10.5194/acp-22-3469-2022, 2022.

Fu, R., Dickinson, R. E., Chen, M. X., and Wang, H.: How do tropical sea surface temperatures influence the seasonal distribution of precipitation in the equatorial Amazon?, J. Climate, 14, 4003–4026, https://doi.org/10.1175/1520-0442(2001)014<4003:HDTSST>2.0.CO;2, 2001.

Guyon, P., Graham, B., Beck, J., Boucher, O., Gerasopoulos, E., Mayol-Bracero, O. L., Roberts, G. C., Artaxo, P., and Andreae, M. O.: Physical properties and concentration of aerosol particles over the Amazon tropical forest during background and biomass burning conditions, Atmos. Chem. Phys., 3, 951–967, https://doi.org/10.5194/acp-3-951-2003, 2003.

Heikenfeld, M., White, B., Labbouz, L., and Stier, P.: Aerosol effects on deep convection: the propagation of aerosol perturbations through convective cloud micro-physics, Atmospheric Chemistry and Physics, 19, 2601–2627, https://doi.org/10.5194/acp-19-2601-2019, 2019.

Heintzenberg, J.: Properties of the Lognormal Particle Size Distribution, Aerosol Science and Technology, 21:1, 46-48, https://doi.org/10.1080/02786829408959695, 1994.

Hernández Pardo, L., Toledo Machado, L. A., Amore Cecchini, M., and Sánchez Gácita, M.: Quantifying the aerosol effect on droplet size distribution at cloud top, Atmos. Chem. Phys., 19, 7839–7857, https://doi.org/10.5194/acp-19-7839-2019, 2019.

Hernández Pardo, L., Machado, L. A. T., Morrison, H.,Cecchini, M. A., Andreae, M. O., Pöhlker, C., Poschl, U., Rosenfeld, D., Vendrasco, E. P., Voigt, C., Wendisch, M., and Pöhlker, M. L.: Observed and simulated variability of droplet spectral dispersion in convective clouds over the Amazon, Journal of Geophysical Research: Atmospheres, 126, e2021JD035076. https://doi.org/10.1029/2021JD035076, 2021.

Holanda, B. A., Pöhlker, M. L., Walter, D., Saturno, J., Sörgel, M., Ditas, J., Ditas, F., Schulz, C., Franco, M. A., Wang, Q., Donth, T., Artaxo, P., Barbosa, H. M. J., Borrmann, S., Braga, R., Brito, J., Cheng, Y., Dollner, M., Kaiser, J. W., Klimach, T., Knote, C., Krüger, O. O., Fütterer, D., Lavrič, J. V., Ma, N., Machado, L. A. T., Ming, J., Morais, F. G., Paulsen, H., Sauer, D., Schlager, H., Schneider, J., Su, H., Weinzierl, B., Walser, A., Wendisch, M., Ziereis, H., Zöger, M., Pöschl, U., Andreae, M. O., and Pöhlker, C.: Influx of African biomass burning aerosol during the Amazonian dry season through layered transatlantic transport of black carbon-rich smoke, Atmos. Chem. Phys., 20, 4757–4785, https://doi.org/10.5194/acp-20-4757-2020, 2020.

Koren, I., Kaufman, Y. J., Rosenfeld, D., Remer, L. A., and Rudich, Y.: Aerosol invigoration and restructuring of Atlantic convective clouds, Geophysical Research Letters, 32, https://agupubs.onlinelibrary.wiley.com/doi/abs/10.1029/2005GL023187, 2005.

Köhler, H.: The nucleus in and the growth of hygroscopic droplets, T. Faraday Soc., 32, 1152–1161, doi:10.1039/tf9363201152, 1936.

Lee, L. A., Reddington, C. L., and Carslaw, K. S.: On the relationship between aerosol model uncertainty and radiative forcing uncertainty, P. Natl. Acad. Sci. USA, 113, 5820–5827, https://doi.org/10.1073/pnas.1507050113, 2016.

Machado, L. A. T., Laurent, H., Dessay, N., and Miranda, I.: Seasonal and diurnal variability of convection over the Amazonia: A comparison of different vegetation types and large scale forcing, Theoretical and Applied Climatology, 78, 61–77, https://doi.org/10.1007/s00704-004-0044-9, 2004.

Machado, L. A. T., Franco, M. A., Kremper, L. A., Ditas, F., Andreae, M. O., Artaxo, P., Cecchini, M. A., Holanda, B. A., Pöhlker, M. L., Saraiva, I., Wolff, S., Pöschl, U., and Pöhlker, C.: How weather events modify aerosol particle size distributions in the Amazon boundary layer, Atmos. Chem. Phys., 21, 18065–18086, https://doi.org/10.5194/acp-21-18065-2021, 2021.

Mattos, E. V., Machado, L. A. T., Williams, E. R., Goodman, S. J., Blakeslee, R. J., and Bailey, J. C.: Electrification life cycle of incipient thunderstorms, J. Geophys. Res. Atmos., 122, 4670– 4697, doi:10.1002/2016JD025772, 2017.

McFarquhar, G. M., Hsieh, T., Freer, M., Mascio, J., and Jewett, B. F.: The characterization of ice hydrometeor gamma size distributions as volumes in N0–λ–μ phase space: Implications for microphysical process modeling, J. Atmos. Sci., 72, 892–909, https://doi.org/10.1175/JAS-D-14-0011.1, 2015.

McFiggans, G., Artaxo, P., Baltensperger, U., Coe, H., Facchini, M. C., Feingold, G., Fuzzi, S., Gysel, M., Laaksonen, A., Lohmann, U., Mentel, T. F., Murphy, D. M., O'Dowd, C. D., Snider, J. R., and Weingartner, E.: The effect of physical and chemical aerosol properties on warm cloud droplet activation, Atmos. Chem. Phys., 6, 2593–2649, https://doi.org/10.5194/acp-6-2593-2006, 2006.

Nyaku, E., Loughman, R., Bhartia, P. K., Deshler, T., Chen, Z., and Colarco, P. R.: A comparison of lognormal and gamma size distributions for characterizing the stratospheric aerosol phase function from optical particle counter measurements, Atmos. Meas. Tech., 13, 1071–1087, https://doi.org/10.5194/amt-13-1071-2020, 2020.

Pöhlker, M. L., Pöhlker, C., Ditas, F., Klimach, T., Hrabe de Angelis, I., Araújo, A., Brito, J., Carbone, S., Cheng, Y., Chi, X., Ditz, R., Gunthe, S. S., Kesselmeier, J., Könemann, T., Lavrič, J. V., Martin, S. T., Mikhailov, E., Moran-Zuloaga, D., Rose, D., Saturno, J., Su, H., Thalman, R.,Walter, D.,Wang, J.,Wolff, S., Barbosa, H. M. J., Artaxo, P., Andreae, M. O., and Pöschl, U.: Longterm observations of cloud condensation nuclei in the Amazon rain forest – Part 1: Aerosol size distribution, hygroscopicity, and new model parametrizations for CCN prediction, Atmos. Chem. Phys., 16, 15709–15740, https://doi.org/10.5194/acp-1615709-2016, 2016.

Pöhlker, M. L., Ditas, F., Saturno, J., Klimach, T., Hrabě de Angelis, I., Araùjo, A. C., Brito, J., Carbone, S., Cheng, Y., Chi, X., Ditz, R., Gunthe, S. S., Holanda, B. A., Kandler, K., Kesselmeier, J., Könemann, T., Krüger, O. O., Lavrič, J. V., Martin,

S. T., Mikhailov, E., Moran-Zuloaga, D., Rizzo, L. V., Rose, D., Su, H., Thalman, R., Walter, D., Wang, J., Wolff, S., Barbosa, H. M. J., Artaxo, P., Andreae, M. O., Pöschl, U., and Pöhlker, C.: Long-term observations of cloud condensation nuclei over the Amazon rain forest – Part 2: Variability and characteristics of biomass burning, long-range transport, and pristine rain forest aerosols, Atmos. Chem. Phys., 18, 10289–10331, https://doi.org/10.5194/acp-18-10289-2018, 2018.

Pöhlker, M. L., Krüger, O. O., Förster, J., Berkemeier, T., Elbert, W., Pöschl, U., Pöhlker, C., Bagheri, G., Bodenschatz, E., Huffman, J. A., Scheithauer, S., and Mikhailov, E.: Respiratory aerosols and droplets in the transmission of infectious diseases, ArXiv: 2103.01188 [physics.med-ph], https://doi.org/10.48550/arXiv.2103.01188, 2021.

Pöschl, U., Martin, S. T., Sinha, B., Chen, Q., Gunthe, S. S., Huffman, J. A., Borrmann, S., Farmer, D. K., Garland, R. M., Helas, G., Jimenez, J. L., King, S. M., Manzi, A., Mikhailov, E., Pauliquevis, T., Petters, M. D., Prenni, A. J., Roldin, P., Rose, D., Schneider, J., Su, H., Zorn, S. R., Artaxo, P., and Andreae, M. O.: Rainforest aerosols as biogenic nuclei of clouds and precipitation in the Amazon, Science, 329 (5998), 1513–1516, https://doi.org/10.1126/science.1191056, 2010.

Reutter, P., Su, H., Trentmann, J., Simmel, M., Rose, D., Gunthe, S. S., Wernli, H., Andreae, M. O., and Pöschl, U.: Aerosol- and updraft-limited regimes of cloud droplet formation: influence of particle number, size and hygroscopicity on the activation of cloud condensation nuclei (CCN), Atmos. Chem. Phys., 9, 7067–7080, https://doi.org/10.5194/acp-9-7067-2009, 2009.

Roesler, E. L. and Penner, J. E.: Can global models ignore the chemical composition of aerosols?, Geophys. Res. Lett., 37, 1–5, https://doi.org/10.1029/2010GL044282, 2010.

Rosenfeld, D., Lohmann, U., Raga, G. B., O'Dowd, C. D., Kulmala, M., Fuzzi, S., Reissell, A., and Andreae, M. O.: Flood or Drought: How Do Aerosols Affect Precipitation?, Science, 321, 1309–1313, https://doi.org/10.1126/science.1160606, 2008.

Seeley, J. T., and Romps, D. M.: The Effect of Global Warming on Severe Thunderstorms in the United States, J. Climate, 28, 2443–2458, https://doi.org/10.1175/JCLI-D-14-00382.1, 2015.

Seinfeld, J. H., Bretherton, C., Carslaw, K. S., Coe, H., DeMott, P. J., Dunlea, E. J., Feingold, G., Ghan, S., Guenther, A. B., Kahn, R., Kraucunas, I., Kreidenweis, S. M., Molina, M. J., Nenes, A., Penner, J. E., Prather, K. A., Ramanathan, V., Ramaswamy, V., Rasch, P. J., Ravishankara, A. R., Rosenfeld, D., Stephens, G., and Wood, R.: Improving our fundamental understanding of the role of aerosol–cloud interactions in the climate system, P. Natl. Acad. Sci. USA, 113, 5781–5790, https://doi.org/10.1073/pnas.1514043113, 2016.

Ulbrich, C. W.: Natural variations in the analytical form of the raindrop size distribution, J. Climate Appl. Meteor., 22, 1764–1775, https://doi.org/10.1175/1520-0450, 1983.

Varanda Rizzo, L., Roldin, P., Brito, J., Backman, J., Swietlicki, E., Krejci, R., Tunved, P., Petäjä, T., Kulmala, M., and Artaxo, P.: Multi-year statistical and modeling analysis of submicrometer aerosol number size distributions at a rain forest site in Amazonia, Atmos. Chem. Phys., 18, 10255–10274, https://doi.org/10.5194/acp-18-10255-2018, 2018.

Williams, M. M. R.: On the modified gamma distribution for representing the size spectra of coagulating aerosol particles, Journal of Colloid and Interface Science, Volume 103, Issue 2, Pages 516-527, ISSN 0021-9797, https://doi.org/10.1016/0021-9797(85)90127-4, 1985.

https://doi.org/10.5194/egusphere-2023-1361
Preprint. Discussion started: 26 June 2023

Wu, W. and McFarquhar, G. M.: Statistical Theory on the Functional Form of Cloud Particle Size Distributions, Journal of the Atmospheric Sciences, 75, 8, 2801-2814, https://doi.org/10.1175/JAS-D-17-0164.1, 2018.

Zhou, J., Swietlicki, E., Hansson, H. C., and Artaxo, P.: Submicrometer aerosol particle size distribution and hygroscopic growth measured in the Amazon rain forest during the wet season, J. Geophys. Res., 107 (D20), 8055, https://doi.org/10.1029/2000JD000203, 2002.